Int. J. Electrochem. Sci., 16 **(2021)** Article ID: 210716, doi: 10.20964/2021.07.22

International Journal of ELECTROCHEMICAL SCIENCE
www.electrochemsci.org

Highly Efficient N-Doped Carbon Quantum Dots for Detection of Hg^{2+} and Cd^{2+} ions in Dendrobium huoshanense

Jun Dai[1], *Peipei Wei*[3], *YujuanWang*[1,2,*]

[1]Anhui Engineering Laboratory for Conservation and Sustainable Utilization of Traditional Chinese Medicine Resources, West Anhui University 237012, Anhui Province, China
[2]Key Laboratory of Biomimetic Sensor and Detecting Technology of Anhui Province, West Anhui University 237012, Anhui Province, China
[3]College of Biological and Pharmaceutical Engineering, West Anhui University 237012, Anhui Province, China
[*]E-mail: 3070714927@qq.com

Received: 21 February 2021 /*Accepted:* 24 April 2021/ *Published:* 31 May 2021

The addition of heteroatoms changes the structure and optical properties of carbon quantum dots (CQDs). In the paper, nitrogen (N)-doped CQDs are prepared via one-step hydrothermal method from Auricularia auricular and ethylenediamine. Transmission Electron Microscope (TEM) analysis reveals that the average size of carbon quantum dots is 5±2 nm, whereas the chemical study shows the existence of C-N bond. The produced N-doped CQDs have fluorescence quantum yields of 28.4%. Moreover, the prepared CQDs showed high sensitivity and accuracy and had a good proportional band of 0-50 μM for detection Hg^{2+} (R^2=0.9919) and Cd^{2+} (R^2=0.9964).The low detection limits were77.21 nM and 101.55 nM for Hg^{2+} and Cd^{2+}, respectively. The CQDs was triumphantly used to track metal ions in environmental samples. So, it was a promising method for environmental pollutant detection.

Keywords: carbon quantum dots, fluorescent probe, detection, dendrobium plant, heavy metal ions

1. INTRODUCTION

CQDs is a new type of fluorescent nanomaterials, which is popular in recent years with diameterless than 100 nm [1-4]. Compared with traditional organic dyes, semiconductors and conventional toxic metal quantum dots, fluorescent CQDs are more effective due to its strong fluorescence emission, excellent optical properties, good biocompatibility and low toxicity, it has been widely used in the fields of analytical detection, biological imaging, drug carriers and chemical sensors, and is a promising fluorescent carbon nanomaterial [5-7]. Due to different raw materials, different hydrophilic characteristic groups (-OH, -NH_2 and -COOH), were formed on their face of CQDs during preparation process, which also makes CQDs have excellent water solubility and easy

surface modification and functionalization. It is one of the environmental friendly fluorescent carbon nano functional materials. CQDs had been synthesized from various natural sources such as orange juice [8], banana juice [9], lemon peel [10], milk [11], rice husk [12], fungus fibres [13], yum [14], orange waste peel [15], egg shell [16], and several other biosources.

Dendrobium huoshanense is one of the first-class national protected plants, and is also an endemic plant in Dabie Mountain of Huoshan County, Anhui Province, and it is a perennial epiphytic herb of orchidaceae. It is the first high-quality and precious Dendrobium species recorded in Shennong herbal classic. It is listed as the first of 'nine immortal herbs in China'. It has the effects of anti-oxidation, anti-tumor, lowering blood pressure, enhancing immunity, protecting liver and stomach. It contains active polysaccharides, amino acids, vitamins, protein, flavonoid, dendrobiol, alkaloid and other compounds [17-23]. Dendrobium houshanense is considered to be the best among Dendrobium because of its long medicinal history and high quality. However, due to its rare wild resources, short plant, slow growth and difficult artificial cultivation, it is difficult to carry out large-scale industrial promotion. Therefore, the improvement of Dendrobium huoshanense has great industrial value. Dendrobium officinale is one of the most widely cultivated medicinal varieties, which is closely related to Dendrobium huoshanense [24].

In recent years, heavy metal pollution incidents occur frequently. Heavy metal pollution has caused a huge threat to the ecological environment and human health, which has also caused widespread concern of the society. Heavy metals can not be biodegraded in organisms, but can be concentrated and enriched thousands of times through the food chain, and finally enter the human body. Heavy metals enter the human body mainly through food, water and atmosphere. Heavy metal contaminated organisms as food into the human body, will accumulate in the body, if long-term consumption, the accumulation of heavy metals in the body more than a certain amount, will cause poisoning. In addition, long-term living in the air polluted by heavy metals or drinking water containing heavy metals can also lead to poisoning. Heavy metal pollution does not only exist in a certain country or region, it has become one of the focuses of international community.

For example, acute tin poisoning can cause nausea, abdominal pain and vomiting lead poisoning can lead to central nervous and brain diseases, mental and intellectual disorders, neurobehavioral abnormalities, and affect children's development, development and IQ, as well as blood anemia and hemolysis. As an essential element of human body, copper is excreted in urine and bile after absorption. However, copper poisoning has been reported in medical literature [25-27].When the concentration of copper in serum reaches 3 mg/L, nausea, vomiting, hemolytic jaundice, renal failure and central nervous system depression may occur. A series of standards for prevention of heavy metal poisoning have been issued, such as GB 11504-1989, which describes in detail the diagnostic criteria and treatment principles of occupational chronic lead poisoning, WS/2112001 formulates the diagnostic criteria for endemic arsenic poisoning, and GBZ 108-2002 formulates the diagnostic criteria for acute metal uranium poisoning. These standards provide a certain guarantee for the prevention of heavy metal poisoning. Detection of heavy metals in food, water, crops and tobacco is of great significance to improve the food safety monitoring system, strengthen the ecological safety assessment in the environment and protect people's life and health. So, it's very important to establish a method with high sensitivity, good accuracy, strong specificity, simple operation and low cost.

In this paper, we produced blue fluorescent CQDs with green non-toxic fungus biomass raw materials (i.e. Auricularia auricula) in the water solvent via muffle furnace high temperature heating method. The effects of N-doped CQDs on the crystal structure and luminescent properties were studied. N-CQDs derived from Auricularia auricula (AN-CQDs) were applied in the field of biosensors, and their preparation, properties and applications were studied. The prepared AN-CQDs perform a vital role in detection of Hg^{2+} and $Cd^{2+}$with high sensitivity in dendrobium plant samples.

2. EXPERIMENTAL PROCEDURE

2.1 Reagents and instruments

All reagents used in this experiment are analytically pure, includingCu^{2+}, Cr^{6+}, Mg^{2+}, Cs^{+}, Cr^{3+}, Ni^{2+}, Hg^{2+}, Pb^{2+}, Ba^{2+}, Cd^{2+}, Mn^{2+}, Co^{2+} and Al^{3+} (Aladdin, Shanghai, China). TEM, TECHNAI G220 S-TWIN instrument, Edinburgh FLS-980 fluorescence spectrophotometer. FTIR, PerkinElmer Spectrum 100. XPS spectra (Thermo Fisher Scientific Inc. U.S.A.), XRD, Bruker D8 Advance, UV-Vis (UV-2600 spectrophotometer, Shimadzu, Japan). Zeta potential meter was used to measure the electromotive potential of CQDs.

2.2 Synthesis of N-Doped CQDs

CQDs from Auricularia auriculawere produced via muffle furnace high temperature heating method. Firstly, Auricularia auricula was powdered, 5 g of Auricularia auricula powder and 2.5g ethylenediaminewere added to 100 mL of distilled water and mixed well, and move into 150mL polytetrafluoroethylene high temperature reactor, the reaction temperature was 200℃, and the reaction time was 12h. After the product was naturally cooled to 20℃, removal of suspended solids by centrifuge (13000 rpm, 16 min), and 0.22 μm microporous membrane was used for further filtration and purification. After the filtrate was evaporated to dryness in vacuum drying oven, golden-yellowaqueous dispersionscontaining N-CQDs were obtained and then stored at 4℃for further use.

2.3 Fluorescence quenching test of Hg^{2+} and Cd^{2+}

50 μLN-CQDs solution and 1 mL PBS were added to the glass tube, mixed and diluted to 3mL. Next, different concentration metal ions were put into centrifuge tube and mixed with vortex for 30s. After standing for 5 min, the fluorescence intensity was determined by fluorescence spectrophotometer, and recorded. The selectivity of detecting metal ions with N-CQDs, different metal ions were selected (Cu^{2+}, Cr^{6+}, Mg^{2+}, Cs^{+}, Cr^{3+}, Ni^{2+}, Hg^{2+}, Pb^{2+}, Ba^{2+}, Cd^{2+}, Mn^{2+}, Co^{2+} and Al^{3+}), the fluorescence detection experiments were developed under the above conditions.

2.4 Analysis in dendrobium plant samples

Extraction and digestion of metal ions from dendrobium plants:dendrobiumplantswere obtained from a local market in Lu'an City, Anhui Province. The dendrobium samples werecrushed with a grinder, passed through a 20 mesh sieve, and stored in a self sealed bag for use. Take 2.00 g of sample powder into a conical flask, put several zeolites, add 10 ml of mixed acid into it, and then cover and soak overnight. Put the conical flask on the electric heating plate for heating and digestion. If the solution turns brown and black, continue to add mixed acid until it emits white smoke. When the digestive solution is colorless and transparent or slightly yellow, stop heating and cool down. When its temperature dropped to 20℃, turn digestive solution to 100 mL volumetric flask, wash the conical flask with a small amount of water for several times, pour the washing solution into the volumetric flask and fix the volume to the scale, mix evenly for standby, and make the reagent blank control.

Then, the fluorescence detection experiments were developed under the above conditions of the metal ions in the actual samples. Different concentration metal ions were added to the samples for spiked fluorescence analysis. The experimental samples needed to be determined for triple, and the recovery and the RSD% should be calculated.

3. RESULTS AND DISCUSSION

3.1 Surface Morphology

Figure 1a, b shows the surface morphology and particle size distributions of N-CQDs. Average diameters for N-CQDs are 5±2 nm, this type of quantum dot has disc-like shape. As shown in Figure 1a, N-CQDs had regular shape, spherical like carbon nanoparticles, no agglomeration phenomenon. The filter size distribution was shown in Figure 1b. The filter size of N-CQDs was between 2.0-8.0 nm, and the average filter size was 5.0 nm.

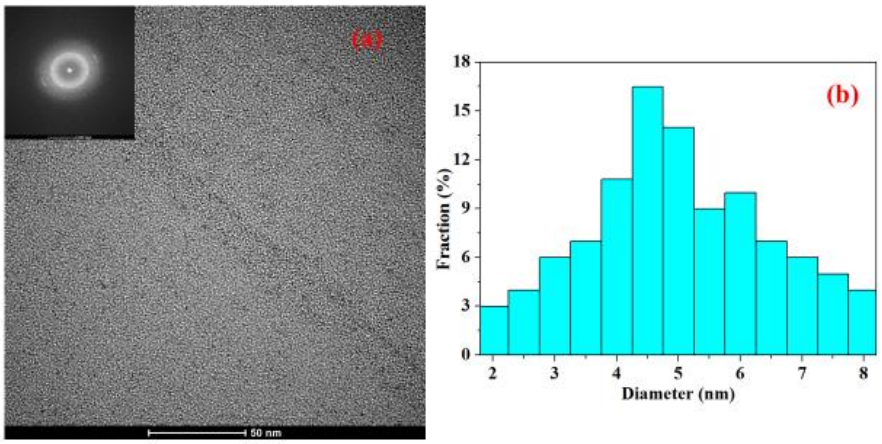

Figure 1. (a) Transmission electronmicroscopy (TEM) images of N-CQDs and (b) average size histogram

3.2 Chemical Composition and Degree of Crystallinity

The characteristic groups on surface of N-CQDs were displayed in Figure 2a by FTIR. The characteristic wavenumber of O-H/N-H was located at 3440 cm^{-1}, the characteristic wavenumber of C=C (called G-band) of sp2 hybrid in C chain and the characteristic wavenumber of C=O are located at 1633 cm^{-1}, 1017 cm^{-1} was C-O-C stretching vibration, which is mainly characterized by disordered structure and surface defect sites (called d-band) [28], which indicates that CQDs had a high degree of graphitization. 1052 cm^{-1} and 2920 cm^{-1} are C-C and C-H stretching vibration.

The surface functional groups and components of N-CQDs were analyzed by X-ray photoelectron spectroscopy (XPS). The characteristic peaks of XPS at 284.0 eV, 398.4 eV and 531.2 eV corresponded to C1s, N1s and O1s, respectively (Figure 2b). In conclusion, the N-CQDs contained C, N, O and other elements, and the surface contains C-N/C-O, C=C, C=O and C-N groups, which had good water solubility.

The crystallinity of N-CQDs was characterized using XRD (Figure 2c), the diffraction peak of N-CQDs was located at 19.7 degrees, indicating that it belonged to amorphous C structure [29, 30].

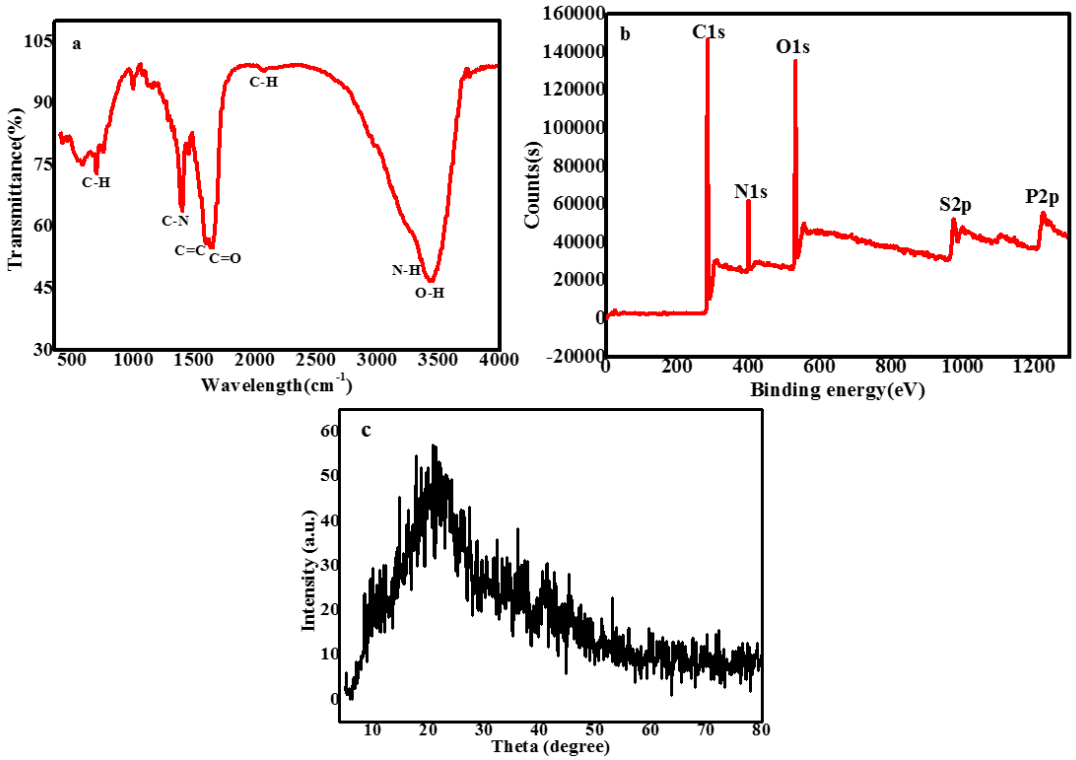

Figure 2. (a) Fourier transform infrared (FTIR) spectrogram of Dendrobium huoshanense carbon quntum dots (N-CQDs), (b) XPS spectra of N-CQDs, (c) X-ray diffractogram of N-CQDs

3.3 UV-Vis and PL Measurements

The N-CQDs had characteristic absorption peaks at λ=278 nm at ultraviolet range, and the empennage extended to Vis-range, as shown in Figure 3a. The behavior was attributed to π-π* transition of C=C bond. The fluorescence of N-CQDs was wavelength dependent, the excitation

wavelength was 350-410 nm, the emission spectrum was red shifted (Figure 3b). As shown in Figure 3a, the maximum excitation wavelength of DH-CQDs was 326 nm and the corresponding emission wavelength was 400 nm. The fluorescence information number of emission spectrum was strong and the stokes displacement was 88 nm, which could avoid scattering. The results shown that the N-CQDs had good fluorescence performance.

According to quinine sulfate, the fluorescence quantum yield of N-CQDs was determined for 23.57%. However, compared to other synthesis procedures, QY of N-doped CQDs produced in our experiment are pretty good [31].

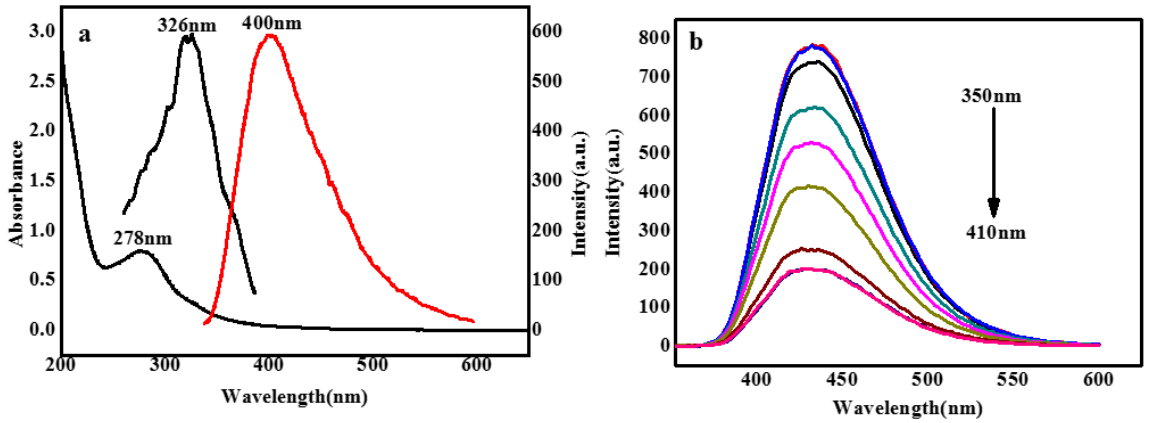

Figure 3. (a) Ultraviolet-visible absorption spectra (blue line),fluorescence excitation at λ=326 nm (black line), and maximum emission (λ=400 nm) (red line) of the prepared N-CQDs, (b) Fluorescence emission spectra of N-CQDs excited at different wavelengths from 350 nm to 410 nm

3.4 Zeta potential Measurements

The Zeta electric potential analyze was used to measure the zeta potential of N-CQDs, Zeta potential was a measure of the strength of repulsion or attraction between particles. The smaller the molecule or dispersed particle was, the higher the absolute value (positive or negative) of zeta potential was, and the more stable the system was, that was to say, dissolution or dispersion could resist aggregation (note that the absolute value of zeta potential represented its stability and positive, negative represented the charge of the particle). It could be seen from Figure 4, the absolute value of zeta potential was 25.2 mV of the N-CODs, which was larger than 25 mV reported in the literature, so the physical stability of the N-CODs was better.

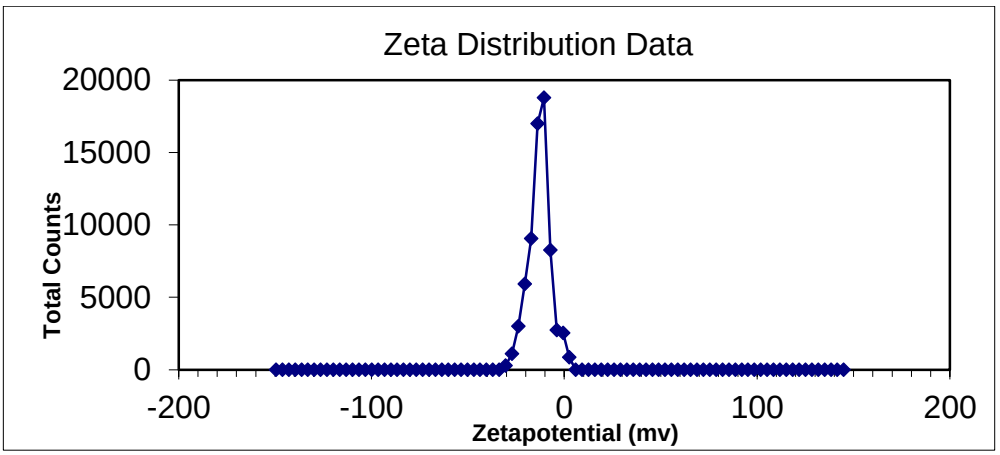

Figure 4. Zeta distribution data of the N-CQDs

3.5 Selectivity of metal ions detection

The selectivity of detecting metal ions by N-CQDs, metal ions such as Cu^{2+}, Cr^{6+}, Mg^{2+}, Cs^{+}, Cr^{3+}, Ni^{2+}, Hg^{2+}, Pb^{2+}, Ba^{2+}, Cd^{2+}, Mn^{2+}, Co^{2+}, Al^{3+} were selected for this experiment. As could be seen from the Figure 5, the fluorescence of N-CQDs could be significantly quenched by $Hg^{2+}$and Cd^{2+}, but other metal ions had no effect on the fluorescence value of the N-CQDs. The results showed that N-CQDs had a high selective response to $Hg^{2+}$and Cd^{2+}, and other metal ions had no interference to the determination of $Hg^{2+}$and Cd^{2+}. Therefore, there was a high selectivity between $Hg^{2+}$and Cd^{2+} and N-CQDs. This demonstrated that N-CQDs could be used to detect $Hg^{2+}$and Cd^{2+}.

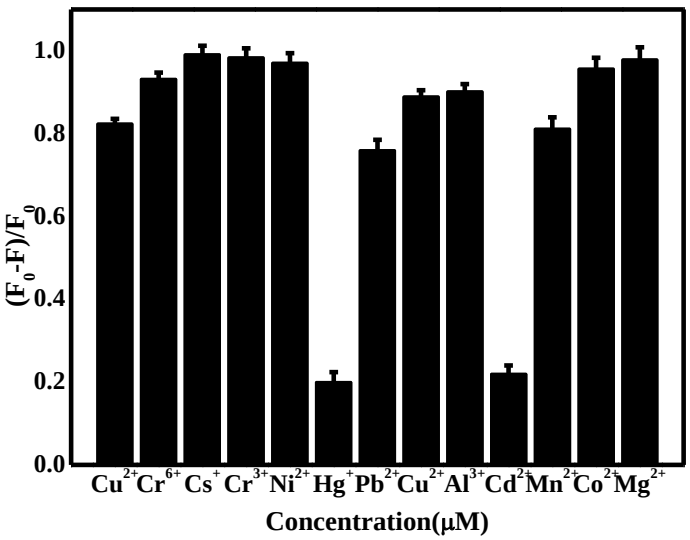

Figure 5. Fluorescence quenching efficiency of different metal ions to the N-CQDs.

3.6 Sensitivity of Hg^{2+} and Cd^{2+} detection

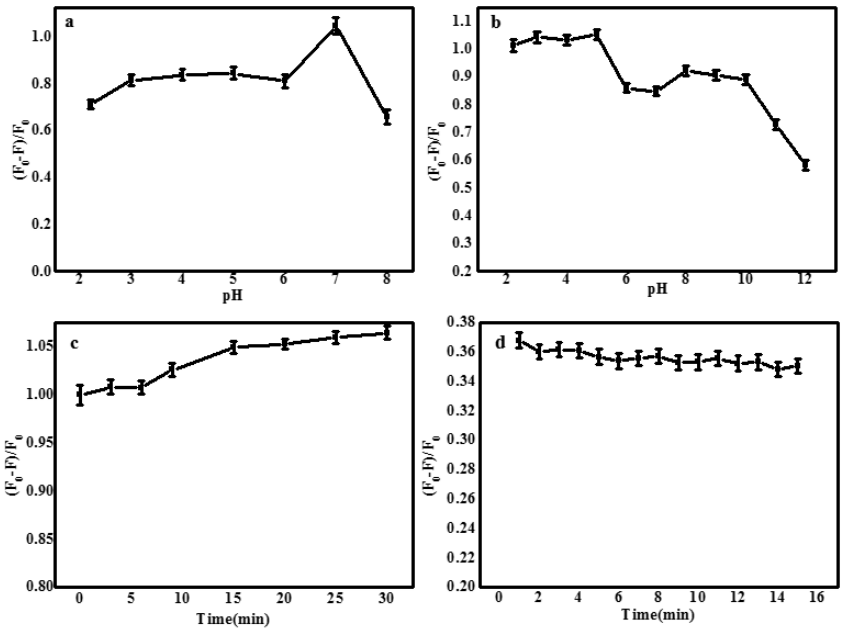

Figure 6. Effect of pH (a, b) and (c, d) reaction time on the fluorescence intensity of the N-CQDs and Hg^{2+} and Cd^{2+}, respectively.

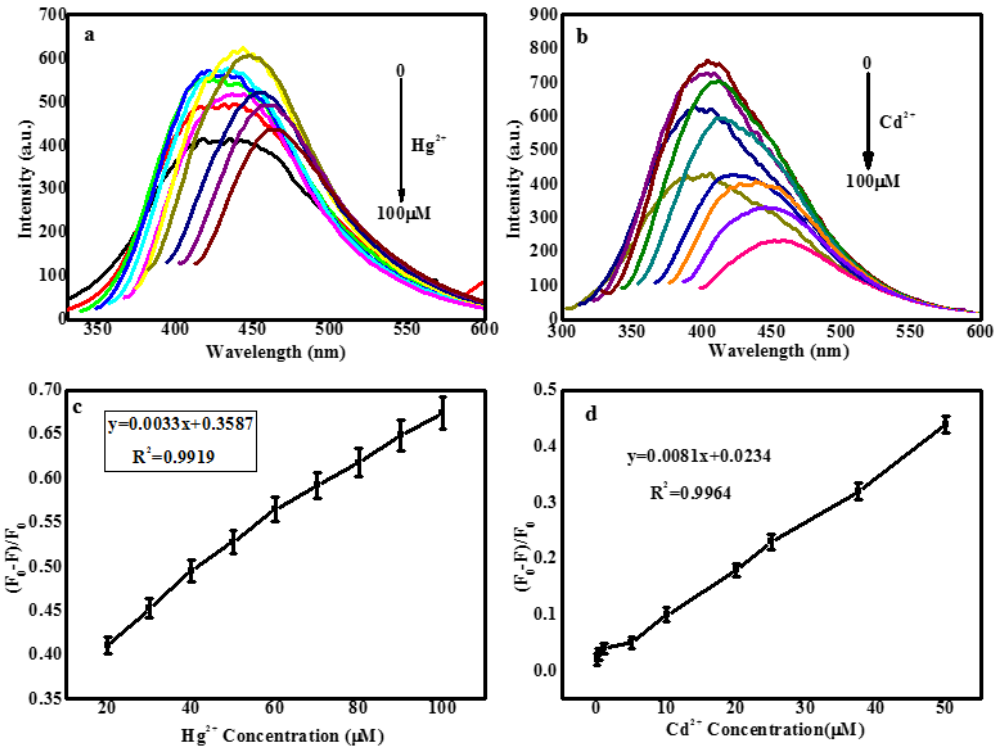

Figure 7. Fluorescence spectra of N-CQDs with various concentrations of Hg^{2+} and Cd^{2+} (0-100 μM) (a, b). Linear relationship between $(F_0\text{-}F)/F_0$ and Hg^{2+} and Cd^{2+} (0-50 μM) (c, d) concentration.

The fluorescence quenching efficiency of N-CQDs for $Hg^{2+}$and Cd^{2+} detection were studied at pH 2.2-12.0. It could be seen from Figure 6a,b, the quenching factor was higher in the range of pH 2.0-4.0 in acid medium, and the fluorescence response is the strongest at pH 7.0, indicating that N-CQDs has the best detection effect for $Hg^{2+}$and Cd^{2+} at pH 7.0. When the pH increased from 8.0 to 12.0, the fluorescence quenching factor decreased gradually. The effect of response time on fluorescence intensity of N-CQDs to detect $Hg^{2+}$and Cd^{2+} were exhibited at Figure 6c, d. The quenching factor of N-CQDs had no obvious change with the increase of time. In this study, the optimum reaction time was 5min.

Under optimal experimental conditions, the variation between the fluorescence intensity and the $Hg^{2+}$and Cd^{2+} concentration were investigated. It could be seen from Figure 7a, b, the fluorescence intensity of the N-CQDs changed regularly with the change of $Hg^{2+}$and Cd^{2+} concentration, respectively, indicating that N-CQDs could be used to trace $Hg^{2+}$and Cd^{2+}. As shown at Figure 7c, d, this method had a fine linear range from 0-50 μM. The equations of Hg^{2+} and Cd^{2+} were F/F_0=0.0033C+0.3587 (R^2=0.9919) and F/F_0=0.0081C+0.0234 (R^2=0.9964), respectively, and it had low detection limits (77.21 nM and 101.55 nM).

3.7 Possible fluorescence quenching mechanism

In recent years, many sensors have been established based on the fluorescence variation of carbon quantum dots. These sensors were primarily analytes that quenched or increased the fluorescence of the carbon dots [32]. Theoretically, this fluorescence phenomenon is related to different mechanisms. For fluorescence quenching, the mechanism is usually divided into dynamic quenching and static quenching, caused by the collision between fluorescent materials and quencher and the formation of ground state complexes respectively [33]. In case of dynamic quenching, the Stern-Volmer equation can be used for analysis [34] with the following formula:

$$F_0/F = 1 + K_q\tau_0 [Q]$$

Where [Q] is the concentration of quencher, F_0 and F are the fluorescence intensity of N-CQDs before and after adding quencher. K_q is the bimolecular quenching constant, τ_0 is the average lifetime of N-CQDs, Generally, the judgment conditions of SQE are as follows [35-37], (1) The fluorescence lifetime of N-CQDs did not change, (2) The formation of the ground state complex changes the absorption spectrum of N-CQDs, (3) The stability of the ground state complex decreases with the increase of temperature, that is, $K_q\tau_0$ decreases with the increase of temperature, (4) The quenching rate constant is greater than 2×10^{10} L • mol^{-1} s^{-1}. In conclusion, the fluorescence quenching mechanisms of Hg^{2+} and Cd^{2+} satisfied the above four points, so it could be concluded that the fluorescence quenching mechanism of this method may be static quenching [38-42].

3.8 Analysis of $Hg^{2+}$and Cd^{2+} in dendrobium plant samples

The above digested dendrobium samples 1-5 were pretreated, and then $Hg^{2+}$and Cd^{2+} in dendrobium samples were detected by prepared N-CQDs. Different concentrations of $Hg^{2+}$and Cd^{2+}

were added to the dendrobium samples for standard recovery experiments, and the same analysis method was used for analysis and detection. The results showed that in Table 1, the recoveries were 80.0~107.7% and the RSD% was 2.35~4.23% (n=3). So, this method was a promising method in the detection of $Hg^{2+}$and Cd^{2+} in dendrobium samples. In addition, as shown in Table 2, the detection limit of this method was higher than that of many previously reported methods for detecting Hg^{2+} and Cd^{2+}. The results showed that the N-CQDs synthesized by this method had high sensitivity for the detection of Hg^{2+} and Cd^{2+}, and could be used for the qualitative and quantitative analysis of Hg^{2+} and Cd^{2+} in actual samples.

Table 1. Analytical results of $Hg^{2+}$and Cd^{2+} in dendrobium samples with N-CQDs (n=3).

Sample	Analytes	Detection (μg/mL)	Spiked (μg/mL)	Found (μg/mL)	RSD (%)	Recovery (%)
sample 1	Hg^{2+}	0.05	2.00	2.04	4.22	80.0
	Cd^{2+}	0.12	5.00	5.11	3.55	91.7
sample 2	Hg^{2+}	0.08	2.00	2.07	3.78	87.5
	Cd^{2+}	0.15	5.00	5.12	4.23	80.0
sample 3	Hg^{2+}	0.09	2.00	2.08	3.64	88.9
	Cd^{2+}	0.20	5.00	5.19	3.28	95.0
sample 4	Hg^{2+}	0.10	2.00	2.09	3.35	90.0
	Cd^{2+}	0.22	5.00	5.20	3.32	90.9
sample 5	Hg^{2+}	0.13	2.00	2.14	2.35	107.7
	Cd^{2+}	0.25	5.00	5.26	2.59	104.0

Table 2. Comparisons of sensing performance of different fluorescent probes for Hg (II) and Cd (II) detection

Fluorescence probes	Linear range (μM)	Detection limit (μM)	References
Polymer Sensor-Hg	1-30	0.728 μM	[43]
N-CQDs[a]-Hg	0-25	0.23 μM	[44]
N-CQDs[b]-Hg	0-18	83.5 nM	[45]
N-CQDs-Hg	0-50	77.21 nM	This work
CDots-Cd	0.1-12	0.03 μM	[46]
N-CQDs-Cd	0-50	101.55nM	This work

[a] N-CQDs: prepared via folic acid as both carbon and nitrogen sources.

[b] N-CQDs: prepared via tartaric acid, citric acid and ethanediamine as the precursors.

4. CONCLUSION

The bright blue fluorescent N-CQDs derived from Auricularia auricula was produced via muffle furnace high temperature heating method. It was introduced about the synthesis of N-CQDs using Auricularia auricula and ethylenediamine as precursors. The structure and characteristic propertiesof N-CQDs were detected by TEM, XRD, XPS, FTIR and UV-Vis. The N-CQDs exhibited

fluorescence emission at 400 nm when excited at 326 nm. The results of N-CQDs antioxidant test emerged non-toxicity, better biocompatibility and fluorescence emission. In addition, $Hg^{2+}$and Cd^{2+} could effectively quench the fluorescence intensity of the N-CQDs. The fluorescence reaction of N-CQDs had a fine linear range in 0-50 μM, under optimal conditions, it had low detection limits (77.21nM and 101.55 nM, respectively). The quenching mechanisms of $Hg^{2+}$and Cd^{2+} on N-CQDs was SQ. Therefore, the method was simple and ideal for metal ions application and high sensitivity detection.

ACKNOWLEDGEMENTS
The subject is supported from scientific research activities of post-doctoral researchers in Anhui Province (2020B453), Postdoctoral research fund project of West Anhui University (WXBSH2019003), Outstanding young talents support program in Colleges and Universities (gxyp2020045), Nature Science Research Project of Anhui Province (1808085QB33), Natural Science Fund of Education Department of Anhui Province (KJ2017A410), (KJ2019A0628).

References

1. M. L Liu, B. B Chen, C. M. Li, C. Z. Huang, *Green Chem.,* 21(2019) 449.
2. R.Wang, K.Q. Lu, Z. R.Tang, Y. J. Xu, *J. Mater. Chem. A.,* 5(2017) 3717.
3. Y. Wang, A. Hu, *J. Mater. Chem. C.,* 2 (2014) 6921.
4. X. Wang, Y. Feng, P. Dong, J. Huang, *Front. Chem.,* 7 (2019) 671.
5. Y. Liu, N. Xiao, N. Gong, H. Wang, X. Shi, W. Gu, L. Ye, *Carbon,* 68 (2014) 258.
6. A. Chae, Y. Choi, S. Jo, N. a. Nuraeni, P. Paoprasert, S. Y. Park, I. In, *RSC Adv.,* 7 (2017) 12663.
7. J. Wang, C. Cheng, Y. Huang, B. Zheng, H. Yuan, L. Bo, M.W. Zheng, S.Y. Yang, Y. Guo, D. Xiao, *J. Mater. Chem. C.,*2 (2014) 5028.
8. S. Sahu, B. Behera, T. K. Maiti, S. Mohapatra, *Chem.Commun.,* 48(2012) 8835.
9. De, B., Karak, N. *Rsc Advances,* 3 (2013) 8286.
10. B. T. Hoan, P. V. Huan, H. N. Van, D. H. Nguyen, V. H. Pham, *Luminescence,* 33(2018).
11. Li, Wang, H. Susan, Z. Zhou, *Anal. Chem.,* 86 (2014) 8902.
12. P. Z. Z. Ngu, S. P. P. Chia, J. F. Y. Fong, S. M. Ng, *New Carbon Mater.,* 31 (2016) 135.
13. C. Shi, H. Qi, R. Ma, Z. Sun, L. Xiao, G. Wei, *ACS Biomater. Sci. Eng.,* 105 (2019) 110132.
14. Z. Zhan, J. Cai, Q. Wang, Y. Su, L. Zhang, Y. Lv, *Luminescence,* 31(2016) 626.
15. P. Surendran, A. Lakshmanan, G. Vinitha, G. Ramalingam, P. Rameshkumar, *Luminescence,* (2020).
16. Q. Wang, X. Liu, L. Zhang, Y. Lv, *Analyst,* 137 (2012) 5392.
17. M. Wei, S. F. Jiang, J. P. Luo, *Chin. J. Biotechnol.,* 23 (2007) 327.
18. H. Wang, N. F. Chen, J. Y. Zheng, *Int. J. Mol. Sci.,* 13 (2012) 16779.
19. X. Q. Zha, J. P. Luo, S. T. Jiang, *Pharm. Biol.,* 45 (2008) 71.
20. M. Massimo, C. Lina, M. Federica, *Food Chem.,* 140 (2013)660.
21. C. C. Chang, A. F. Ku, Y. Y. Tseng, *J. Nat. Prod.,*73 (2010)229.
22. X. Xing, S.W. Cui, S. Nie, *Bioact. Carbohydr. Dietary Fibre,* 1 (2013) 131.
23. J. C. Ge, X. Q. Zha, C. Y. Nie, *Carbohydr.Polym.,* 189 (2018) 289.
24. J. Luo, B. W. Hou, Z. T. Niu, *PLoS One,* 9(2014) 99016.
25. B. Qiu, C. Xu, D. Sun, *Acs Sustainable Chem. Eng.,* 2 (2014) 2070.
26. M. Shirzadsiboni, M. Farrokhi, R. D. C. Soltani, *Ind. Eng. Chem. Res.,* 53 (2014) 1079.
27. Y. H. Jiang, W. Q. Cai, W. J. Tu, *J. Chem. Eng. Data,* 64 (2019) 226.
28. F. Karlicky, K. K. RamanathaDatta, M. Otyepka, R. Zboril, *ACS Nano,*7 (2013) 6434.
29. P. Wu, W. Li, Q. Wu, Y. Liu, S. Liu, *RSC Adv.,* 7 (2017) 44144.

30. T. N. J. Edison, I. R. Atchudan, M. G. Sethuraman, J. J. Shim, Y. R. Lee, *J.Photochem. Photobiol.,B,* 161 (2016) 154.
31. Z. Li, D. Wang, M. Xu, J. Wang, X. Hu, S. Anwar, A. C. Tedesco, P. C. Morais, H. Bi, *J. Mater. Chem. B*, 8 (2020) 2598.
32. A. Mariappan, K. Kaviyarasu, K. Neyvasagam, A. Ayeshamariam, P. Pandi, R.R. Palanichamy, C. Gopinathan, G.T. Mola, M. Maaza, *Surf. Interfaces*, 6 (2017) 247.
33. K. Kaviyarasu, K. Kanimozhi, N. Matinise, C. Maria Magdalane, G.T. Mola, J. Kennedy, M. Maaza, *Mater. Sci. Eng., C*, 76 (2017) 1012.
34. Y. Guo, L. Zhang, S. Zhang, Y. Yang, X. Chen, M. Zhang, *Biosens. Bioelectron.* 63 (2015) 61.
35. J.R. Lakowicz, Principles of Fluorescence Spectroscopy, 3rd. ed., Springer, Singapore, 2006.
36. X. Sun, Y. Wang, Y. Lei, *Chem. Soc. Rev.*, 44 (2015) 8019.
37. M. Formica, V. Fusi, L. Giorgi, M. Micheloni, *Coord. Chem. Rev.*, 256 (2012) 170.
38. P. Zuo, X. Lu, Z. Sun, Y. Guo, H. He, *Microchim. Acta*, 183 (2016) 519.
39. C. S. Xiang, L. Yu, TrAC, *Trends Anal. Chem.*, 89 (2017) 163.
40. J. S. Wu, W. M. Liu, J. C. Ge, H. Y. Zhang, P. F. Wang, *Chem. Soc. Rev.,* 40 (2011) 3483.
41. Y. Liu, W. Duan, W. Song, J. Liu, C. Ren, J. Wu, D. Liu, H. Chen, *ACS Appl. Mater. Interfaces*, 9 (2017) 12663.
42. Y. Liu, Y. Zhao, Y. Zhang, *Sens. Actuators, B,* 196 (2014) 647.
43. J. Li, Y. Wu, F. Song, *J. Mater Chem.*, 22 (2011) 478.
44. R. Zhang, W. Chen, *Biosens. Bioelectron.*, 55 (2014) 83.
45. H. Huang, Y. Weng, L. Zheng, *J. Colloid Interface Sci.*, 506 (2017) 373.
46. R.Vaz, J. Bettini, J.G.F. Júnior, E.Lima, W. G.Botero, J. Santos, *J. Photoch. Photobio. A.*, 346 (2017) 502.